Article

Designing Wind Energy Harvester for Connected Vehicles in Green Cities

Zuhaib Ashfaq Khan [1], Hafiz Husnain Raza Sherazi [2]*, Mubashir Ali [3], Muhammad Ali Imran [4,5], Ikram Ur Rehman [2], Prasun Chakarbarti [5]

1 Department of Electrical Engineering, COMSATS University Islamabad, Attock Campus, Punjab, Pakistan
2 School of Computing and Engineering, University of West London, London, United Kingdom
3 Dept. of Management, Information and Production Engineering, University of Bergamo, Bergamo, Italy.
4 School of Engineering, University of Glasgow, Glasgow, United Kingdom.
5 Artificial Intelligence Research Centre (AIRC), Ajman University, Ajman, UAE.
6 Techno India NJR Institute of Technology Udaipur 313003 Rajasthan, India
* Correspondence: sherazi@uwl.ac.uk

Abstract: The recent advancements in the field of communication have led data sharing to become an integral part of today's smart cities with the evolution of concepts such as the internet of vehicles (IoV) paradigm. As a part of IoV, Electric Vehicles (EVs) have recently gained momentum as authorities have started expanding their Low Emission Zones (LEZ) in an effort to build green cities with low carbon footprints. Energy is one of the key requirements of EVs not only to support the smooth and sustainable operation of EV itself but to also ensure connectivity between the vehicles and infrastructure with controlling devices like sensors and actuators installed within an EV. In this context, renewable energy sources (such as wind energy) dramatically play their parts in the automobile sector towards designing the energy harvesting electric vehicles (EH-EV) to pare the energy reliance on the national grid. In this article, a novel approach is presented to achieve electric generation due to vehicle mobility to support the communication primitives in electric vehicles which enables plenty of IoV use cases in the presence of surplus energy at hand. A small-scale wind turbine is designed to harness wind power for converting it into mechanical power. This power is then fed to the onboard DC generator to produce electrical energy. Furthermore, the acquired power is processed through a regulation circuitry to consequently achieve the desired power supply for the end load, i.e. the batteries installed. The suitable orientation for efficient power generation is proposed on ANSYS-based aerodynamics analysis. The voltages induced by DC generator at No-Load condition are 35V while at Full-Load 25V are generated at rated current of 6.9A, along with the generation of power at around 100W (at constant voltage) at the rated speed of 90 mph for nominal battery charging. Moreover, the acquired data can be monitored via an android application interface by using a Bluetooth module.

Keywords: Energy Harvesting; power management, Connected Vehicles; wind energy harvester; Smart Cities; electric Vehicle; IoT; Tesla; autonomous sensors

Citation: . *Preprints* **2021**, *1*, 0. https://doi.org/

Received:
Accepted:
Published:

1. Introduction

Vehicular Adhoc Networks (VANET) [1,2] can genuinely be viewed as a game changer in repainting the future of electric vehicles. The incorporation of the concept of 5G communication modes is also in wide discussion. These communication paradigms have opened up a broad spectrum of technological advancements such as VANET [3,4], IoV [5–7], and industrial automation [8,9] to name a few. The IoV not only promotes connectivity to achieve communication among the vehicles, but also with the road side infrastructure that promotes its safety and ease of service on the road. This encourages the advancement in IoT, which focuses on concept of strong telecommunication services as well as better control and safeguard of household and working areas, paving way for concepts such as smart cities [10] and smart grid. These practices are also developing new ideas in the field of Industrial automation, promoting a new generation of robotics and automated control systems for efficient production. These innovations are creating a surge of electric power consumption in the near future, which requires more hands on methods for energy generation.

The constantly increasing carbon emissions caused by the conventional gas powered vehicles have led the research efforts toward the inception of Electric Vehicles (EV) [11–13], being one of the greatest inventions of recent decades. The concept started to took an implementation form in the early 21st century. The practical concept of the electric vehicle was introduced to the world by Tesla Co.. The car runs on electric batteries which turn a motor in the car that rotates the axle shaft of the accelerator wheels. The technology has since modernized the automobile industry, but its range and charging is still an issue to be revolutionized. The EV's get charged from static charging ports. These charging ports will get electricity from the power plants which are already supplying electric power to all types of loads i.e. residential, commercial, industrial, etc. When the EV's will rely upon those power stations, there will be a huge increase in electricity demand. So, there is a need for a mobile charging system for the EV's to reduce their dependence upon the power plants, and also if the battery gets completely used, there should be a way of providing electric power to the vehicle.

Several techniques have been introduced for electricity generation from moving vehicles with fans mounted on different positions i.e. using windmill mounted on trunk and top of car and train but some issues were still in the way for effective generation, like previous researches were not compatible with every vehicle and they directly relied on output power of the fan i.e. there was no work done on electrical side. In the first concept for charging the car in mobility demonstration [14], a wind turbine is mounted on the top of the car to charge the car's battery using the wind energy striking on the car. The practical results had drawback of an increase of drag force on the car that effected the efficiency of the car [15]. Then, a Malaysian researcher group shows with the help of simulation the cause of that increase in the pressure on the car [16]. The simulation showed that the front and the bonnet of the car is much more reliable for mounting the wind turbine than the top [17]. So, for that reason we are trying to prove the hypothesis given in the previous work by mounting a wind turbine on the front of the car for electricity generation. Another attempt to make a vehicle-mounted wind turbine system was made [18], they mounted a miniaturized wind mill [19] on the back of a pickup truck but the design had a flaw for not being applicable for every other type of cars [20,21].

The approach is to mount a wind turbine on the front of the car. When the car is in motion, the air will create a significant force on the car (as well as the turbine). This forceful air will go through the blades of the fan. The wind will produce torque and causing the blades to rotates and as a result, kinetic energy will be produced. This kinetic energy from the turbine is transferred to the rotor shaft of the electric generator, creating an electric induction. As a result of this induction, electricity is generated. The amplitude of the generated voltages depend upon the number of rotations (RPMs) of the rotor. As the system is used for DC batteries [22] charging, DC generator [23] is used to generate DC voltages are generated but there is a range of DC voltages. An issue arises that the battery of the electric vehicle needs to be charged at constant voltage, so for this purpose a DC stabilizer [24] is used to stabilize the range of DC voltages generated by the DC motor. So, the DC voltage stabilizer will stabilize/regulate the range of DC voltages to a specific DC voltage for different batteries (Li-ion [25] or lead acid [26]), but will allow the maximum current to pass through it for battery charging. The general concept of the research analysis is shown in Figure 1.

The remainder of this research work is organized as follows. In Section 2, the overall system design is introduced. In Section 3 the complete methodology, working of the system model and the Bluetooth module monitored application is discussed. The result analysis is presented in Section 4, while in the section 5 a complete system efficiency analysis is presented, followed by the conclusion made in Section 6.

Preprints (www.preprints.org) | NOT PEER-REVIEWED | Posted: 9 July 2021 doi:10.20944/preprints202107.0214.v1

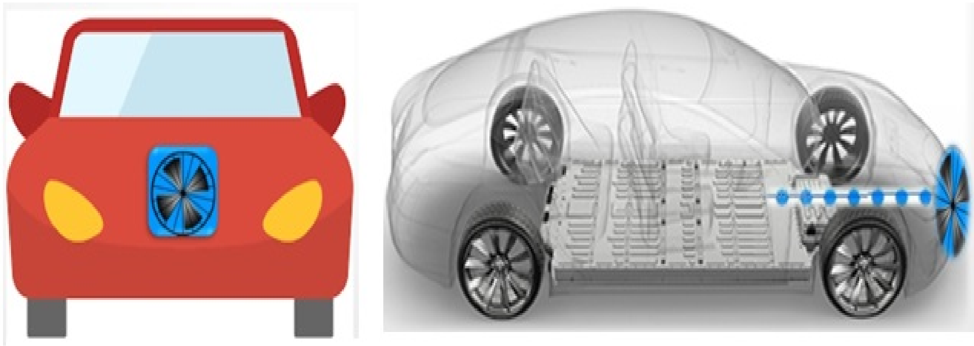

Figure 1. Fan mounted (left), electrical generation (right)

2. System Model

A sequential model of the system design is shown in Figure 2 given below. The basic step is the extraction of wind using fan blades, connected with the PMDC motor which generates electricity upon the rotation of its shaft primarily caused by the collision of wind. The motor is connected with DC regulator which provides a regulated DC output to the battery. This output is measured using voltage sensor[27] and current sensor connected with Arduino. There is an LCD screen connected with the Arduino to display the electrical parameters of the regulated output. Then the next phase is the protection circuitry which has two functions. One is the switching of electric power using a relay module[28] being controlled by Arduino and decision taken upon the basis of percentage of charge ratio of the battery. The other function of protection circuitry is to stop the flow of current from battery towards the motor by using power diode[29]. After this, the electrical power is provided to the battery for getting charged. There is a Bluetooth module connected with Arduino to display the electrical parameters (voltage and current) on the mobile application.

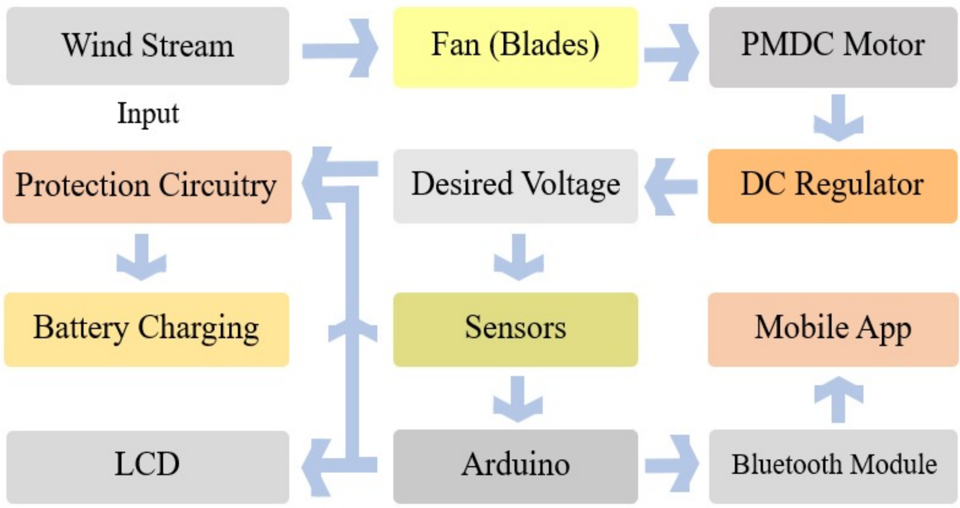

Figure 2. System Block Diagram

The architecture of the proposed model is demonstrated in Figure 3. The first part of the system is fan which is being used to convert the energy of wind into kinetic energy of the blades. This fan is connected with the shaft of permanent magnet DC (PMDC) motor which, in turn, will rotate it. The DC motor will act as a generator that will generate electricity upon the rotation of its shaft. This generated electricity will be measured by using voltage and current sensors[30] in parallel and series, respectively. The output of the DC motor will be fed to the DC regulator which regulates the generated output voltage. The output

 doi:10.20944/preprints202107.0214.v1

of the DC regulator is again measured using voltage and current sensors so as to calculate the voltage and current respectively and thus power. In this way, the input and output electrical parameters of DC regulator are used to measure the efficiency of the regulator. After this, there will be a protection circuitry installed which contains a relay module and a diode. Arduino continuously measures the voltage across the battery to calculate the percentage up to which the battery has been charged. Based on this calculation, the Arduino will decide whether to switch on the relay or not. If the voltage across the battery is between minimum and maximum set voltages, the relay will be switched on, otherwise it will be off. In VANET perspective[31,32], a mobile app operated via a Bluetooth module is also designed which enable us to get the results of the electric generation on the app for easy access to the data. Finally, the diode before the battery will allow current to flow only towards it and will stop current to move in the other direction.

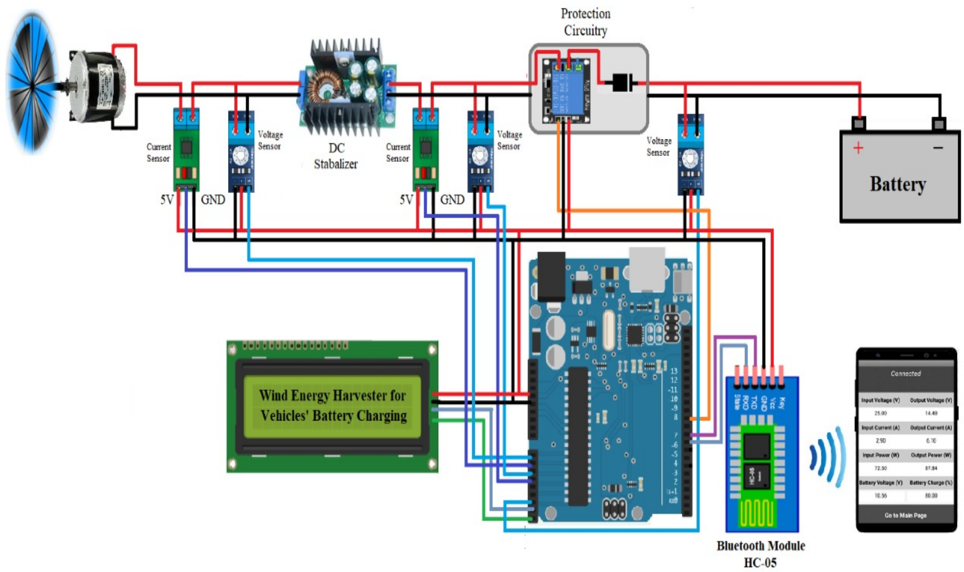

Figure 3. Proposed Architecture of the system

2.1. Mathematical Modeling

To make a charging system, certain parameters of the car and the electric unit for the production of the charging is required. From the mechanical aspects to the electrical parameters of the car charging system, a complete mathematical modeling of the system is required. The mathematical model of the system can be seen in the Figure 4.

For the calculations of various stages of power generation, the key parameters required for are the cross-sectional area of the fan, which expresses the wind that will act on this surface for turbine rotation. Under vehicle's structural limitations the bigger the area is, the larger exertion of air pressure will be there. The second one is the air velocity, that will be acting on the car due to the change of car speed. The faster the car, the higher air velocity will be present.

2.1.1. Wind/Turbine Power

The air traveling with some velocity will exert kinetic energy on the turbine. So by using the equation (1) K.E of the system can be calculated, now the turbine power generated from air depends upon the mass flow rate of air which is expressed in equation (2), Where ρ is the density of air, A is the area of cross section of turbine and v is the air velocity[33]. Now, the turbine power is equal to the kinetic energy exerted by air given in equation (3). The formula for the power generated by the turbine via wind power[34] is given in

Preprints (www.preprints.org) | NOT PEER-REVIEWED | Posted: 9 July 2021 doi:10.20944/preprints202107.0214.v1

Maths.png

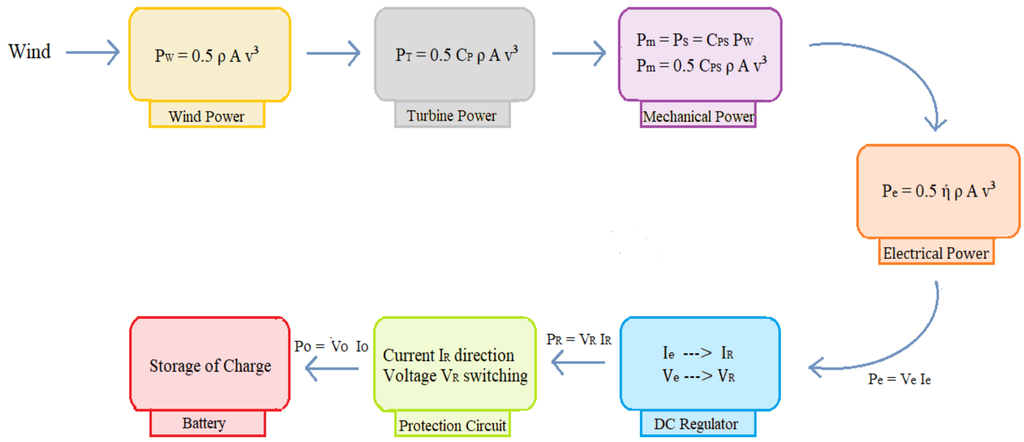

Figure 4. Mathematical Model

expressed in equation (4), where P_r is the turbine power and C_P is the power coefficient for the turbine.

$$KE = \frac{1}{2}mv^2 \tag{1}$$

$$m = \rho A v \tag{2}$$

$$KE = \frac{1}{2}\rho A v^3 \tag{3}$$

$$P_r = \frac{1}{2}C_P \rho A v^3 \tag{4}$$

2.1.2. Mechanical Power

In order to find the shaft power, the first thing we need to determine is the shaft power coefficient. For that we first need to determine the tip to speed ratio of the shaft which is determined by formula:

$$\lambda = \frac{4\pi}{B} \tag{5}$$

Where B(=7) is the number of blades.
$\lambda = \frac{4\pi}{7} = 1.795$
from the graph below as shown in Figure 5, the $\lambda = 1.795$ correlates to a power coefficient: C_P=0.13
With an augmentation of 0.2, C_{P_s} = 0.13 + 0.21 = 0.34, where C_{P_s} is the shaft power coefficient. Now, the mechanical power is equal to the shaft power that is:

$$P_{mech} = P_s = C_{P_s} P_w = \frac{1}{2}C_{p_s}\rho A v^3 \tag{6}$$

For the turbine diameter of 0.36m, the area of turbine is determined by formula:

$$A = \frac{\pi d^2}{4} \tag{7}$$

2.1.3. Electrical power

The shaft power induced in the shaft of the generator is transmitted to the generator for induction process. This induction is responsible for the generation of electric power. The formula is given in given in equation (8), where η is the net efficiency of the generator. As power in is corresponding to (speed and torque) and power out is relative to (speed and

Preprints (www.preprints.org) | NOT PEER-REVIEWED | Posted: 9 July 2021 doi:10.20944/preprints202107.0214.v1

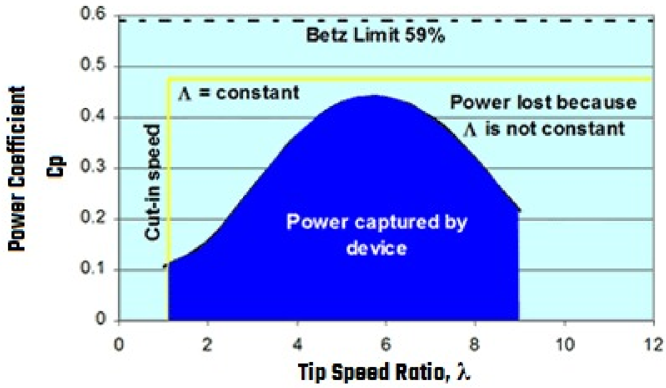

Figure 5. Tip speed ratio vs Power Coefficient[14]

current) then the torque mechanical applied is relative to the current being drawn by the windmill. The torque on the rotor can be calculated by the formula of equation (9), Where T is the torque and ω is the angular velocity of the rotor. the ω can be calculated by the formula given in equation (10), where R is the length of the fan blade.

$$P_{elec} = \frac{1}{2}\eta\rho A v^3 \tag{8}$$

$$P_s = T\omega \implies T = \frac{P_s}{\omega} \tag{9}$$

$$\omega = \frac{\lambda v}{R} \tag{10}$$

2.1.4. RPMs and Angle of Twist

The blade angle of twist is the angle at which blades are set to accumulate the maximum air pressure for effective generation, where N is the rotational speed of the rotor given in revolutions per minute(rpm)[35], which can be calculated through the formula in equation (11).

$$N = \frac{60\lambda v}{2\pi R} = \frac{60 * 1.795 * 33.33}{2 * \pi * 0.18} = 3174rpm. \tag{11}$$

2.1.5. Force Calculation

The force acting on the fan to operate is the difference of two forces acting on it. One is the lift force(F_L),that is exerted by the air to rotate the fan expressed in equation (12).

$$F_L = \frac{1}{2}C_L\rho V^2 A_t \tag{12}$$

but for every action, and opposite reaction is present. in this case an opposite force emerges which tries to restrict the fan from moving. This force is called drag force and is calculated by the following formula in equation (13).

$$F_D = \frac{1}{2}C_D\rho V^2 A_t \tag{13}$$

where C_L and C_D are the lift coefficient and drag coefficient respectively, and A_t is the fan surface area. Now, the total force on the fan is the vectorial sum of both forces.i.e.

$$F = F_L\cos(90-\phi) - F_D\sin(90-\phi) \tag{14}$$

3. Methodology

As this research work brought novelty in the technology so there was a need to propose its design on the basis of new analysis to be conducted. Thus, first of all, software based simulations were used to take decisions regarding the hardware of the system. After this, the complete schematic was designed and hardware was implemented. The components have been connected in accordance with the proposed schematic. First of all is the wind turbine, whose output is given to the DC voltage regulator, having current and voltage sensors on its input and output. The output of the DC voltage regulator is connected to the battery with a protection circuitry in its way. This protection circuitry is used to protect the battery from over-charging and low charging, by switching the circuit ON and OFF at suitable time. This decision is taken by Arduino. Moreover, this protection circuitry also stops the flow of current back from the battery towards the wind turbine. After this hardware was designed, implemented and tested for its working and it was assured that this hardware now ready to be used practically, it was then implemented on car. In the Figure 6(a), it can be seen that the fan has been mounted on the front of the car. Only fan is out of the car body. The reason is that there is a need of air to strike the fan to rotate it and no other component is necessary to be mounted outside the car body. So, the Permanent Magnet DC (PMDC) Motor has been placed inside the car body. The reason of placing the car motor inside the car body is that there should neither be type of weight with fan outside the car nor there should be any drag force due to this placement of motor. The output of the DC motor has been connected to the rest of the circuit using DC wires, suitable for carrying the current through it, from inside the car engine. Another view of the fan, mounted outside the car, can seen in the Figure 6(b). After generation of electricity from

(a) (b)

Figure 6. Car mounted fan

the wind turbine, the output is being transmitted to the battery after it is being stabilized, measured and the protection is assured. The DC wires will take this electricity towards the rest of the system, which is placed inside the car. In the Figure 7 below, it is shown that the input is being given to the system for regulation, measurements and protection work. After which the output is being given to the battery for getting charged.

3.1. Bluetooth Monitoring via Android App

In a research work, where something is being measured or calculated, there is a need to display it. As in this research article, the data was displayed in LCD using Arduino. Still, there was a need to have a display that should be user friendly. Hence, an Android App has been developed using the MIT App Inventor, which will display the input and output electrical parameters and also the battery percentage. This data is being sent to a mobile phone from Arduino via Bluetooth connection using a Bluetooth Module, HC-05.

 doi:10.20944/preprints202107.0214.v1

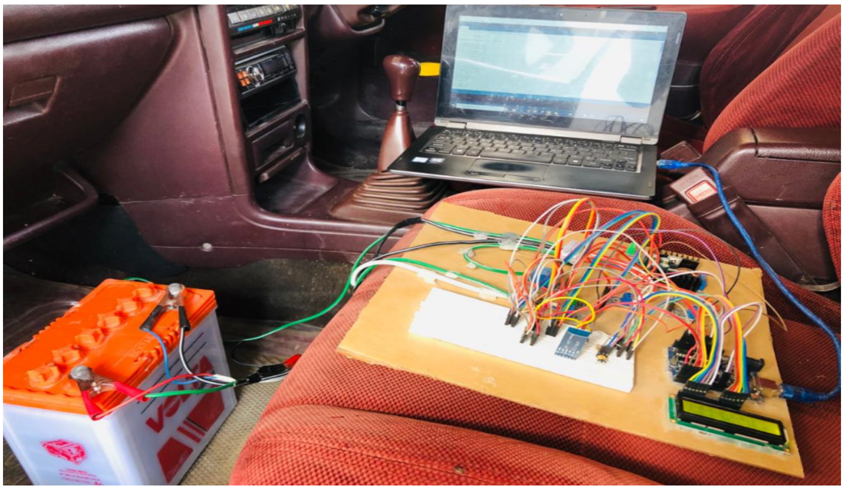

Figure 7. Hardware system implemented in car

This objective of the research work has been done after achieving all the milestone of the article and therefore takes this work to two different technologies:

3.1.1. Mobile Monitoring

In this research work, the car is being driven and a wind turbine is being used to generate electricity. This electricity is being measured and displayed on an LCD using Arduino. Furthermore, this data is being sent to the mobile phone of the user to be displayed there in an Android App, as shown in Figure 8. This mobile monitoring is being achieved using Bluetooth connection between the Arduino and the mobile phone.

3.1.2. Human-Machine Interface

As the measured data is being displayed on the user's mobile phone, it has to be made user-friendly. In this Android App, that will be installed on the mobile of the user, the user will be able to open the introductory part of the app, in which he/she will be able to see the author's team and also watch the Demo Video of the work. Moreover, the user will be able to connect the mobile to Arduino and start receiving the information from Arduino via Bluetooth.

4. Results and Discussion

4.1. Simulation Results

For performing software analysis, affect of air on car has been simulated by using ANSYS workspace 16.0 [36,37] for the evaluation of aerodynamic properties for the execution of our research. Software analysis helps us to grasp the idea of the affect of air velocity on the car as well as various zones of drag coefficient present around the vehicle. For the evaluation of the air velocity and drag force, fluent module of ANSYS has been used, in which different analysis techniques have been used.

4.1.1. Iteration Analysis

In this simulation analysis, the geometry of an EV is included in Fluent to perform some analysis techniques. This simulation done for this research work is done at 200 iterations at a speed of 35m/s, which is the maximum speed at which the vehicles are driven in general. In this type of technique, an air thrust is exerted on a car in the entire axis (X, Y, and Z-axis) of the vehicle. The x-axis shows the number of iteration and along the y-axis is the scale for the residual air-stream on each coordinates of the vehicle.

Preprints (www.preprints.org) | NOT PEER-REVIEWED | Posted: 9 July 2021 doi:10.20944/preprints202107.0214.v1

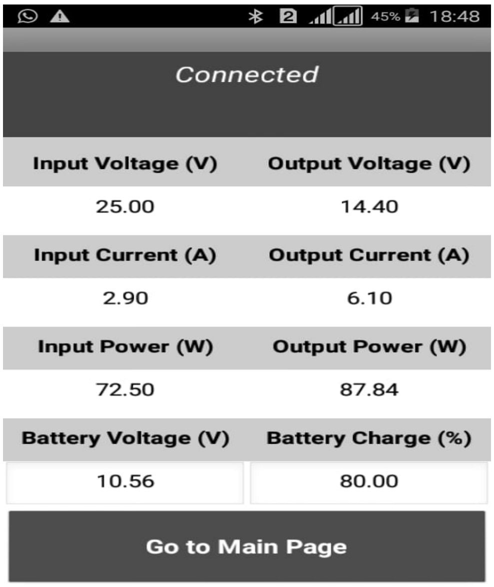

Figure 8. Measurements being displayed on App

4.1.2. Pathlines Analysis

This concept is further expanded via running multiple iterations of the same air model using vectors graphical method. This gave us a comprehensive look of the effect of air on the car. As shown in the simulation in Figure 9, it shows in which region the drag force is strongly present and where its presence is negligible. This indicates that when a car model is made, priority is given to the aerodynamics of the car for effectively resisting the drag force. The Figure 9 also shows that with how much velocity does the air strike the car when it is being driven. It can be seen that there are small lines showing the flow of air towards the car and their colour indicates the air velocity on the surroundings of the car. It is clear that on the front, there is enough air velocity on the front of the car, necessary for the system to work properly. Too much air velocity is not required by the system as there remains a risk of its damage by too much pressure. Thus, the air velocity on the front is enough.

4.1.3. Contours Analysis

In the next simulations using the contours graphical method which counts the surface area using different iterations, a complete structural analysis has been done to identify the effectiveness of the air velocity on the vehicle. In Figure 10(a) the front as well as sides are easily visible and indicate that the front of the EV directly confronts the maximum air as compared to the other parts of the body and sides are the second most pressure tolerant region of the car. Basically, this analysis is done in accordance with the shape of the car which shows that on which parts of the car, there will be more pressure exerted by the wind when the car will be driven. It can be seen that when a car is driven then due to its direct contact with the wind, there is maximum pressure being exerted. Moreover, on the wind screen and other parts also get a considerable amount of pressure. Another view of the same analysis can be seen in Figure 10(b) where it is clear that the parts of the car which are vertical in shape get more pressure by the wind and so on.

4.1.4. Velocity Pathway Simulation

In this simulation analysis in Figure 11(a), the air velocity acting on the car's body is evaluated. It is seen that most of the air resistance passes around the car smoothly, while the front blocks and directly confronts the air acting on it. As it is seen that the maximum air velocity is on the top of the car body but this location is not feasible for mounting a diffuser on the roof of the car because this will increase the weight of the vehicle. So, keeping this point in mind, a system has been proposed which can be adjusted on the front bumper of the car where the air velocity is according to our system needs. Basically, this analysis also tells us about the drag force on various parts of the vehicle. Now, when this analysis is carried out on a vehicle, it shows that when the air strikes the car then obviously it has to pass across it, in order to keep the vehicle moving. This analysis tells us about the air which passes along the vehicle. In Figure 11(b), it can be seen that after striking the car, most of the air is moving either from above the car or from it's beneath. Hence, there is less drag on the front of the car, as the scale on the left side depicts. So, front of the car is a suitable location for the wind turbine to be mounted.

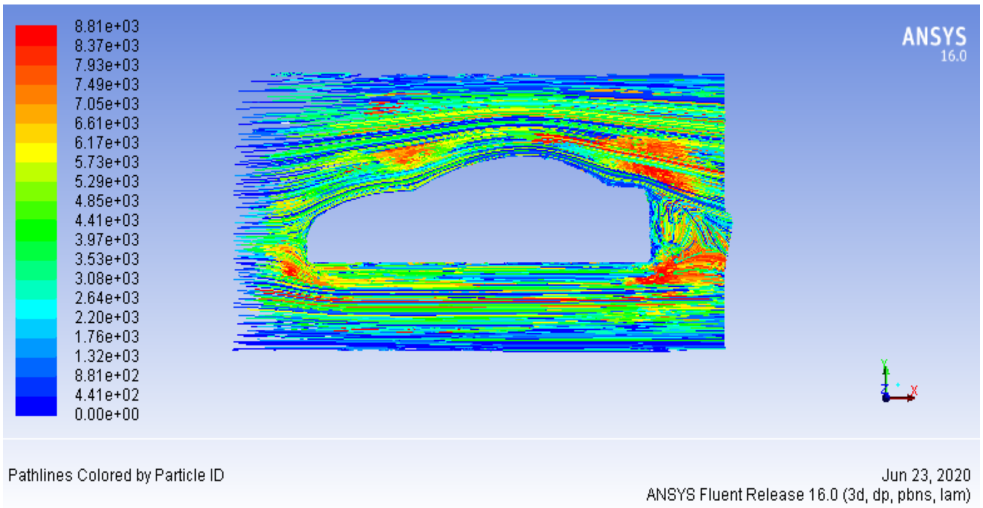

Figure 9. Air Flow Path-lines

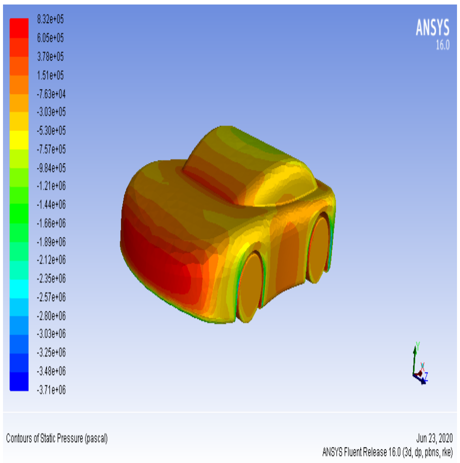

(a)

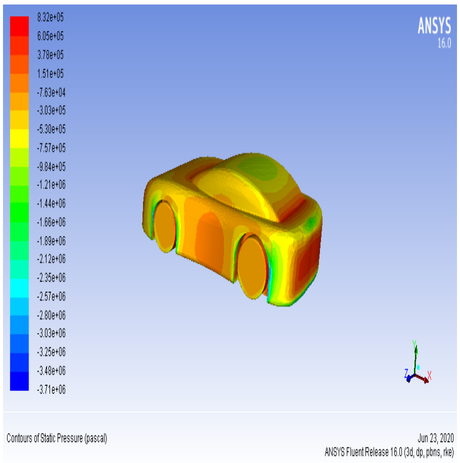

(b)

Figure 10. Contours effects

4.2. Testbed Results

4.2.1. Car Speed vs Air Velocity

At first, calculations were made on practical basis to help us clarify the difference between the vehicle's velocity vs the air velocity on it. This was so that we can clarify the fact that at the designated location, the air velocity is ample enough to run the wind generator's fan blades. The relation between them can be see in the Figure 12, which confirms that the air velocity is slightly less to allow the car to run but has enough kinetic energy to be provided to the generator to generate momentum for the fan blades.

 doi:10.20944/preprints202107.0214.v1

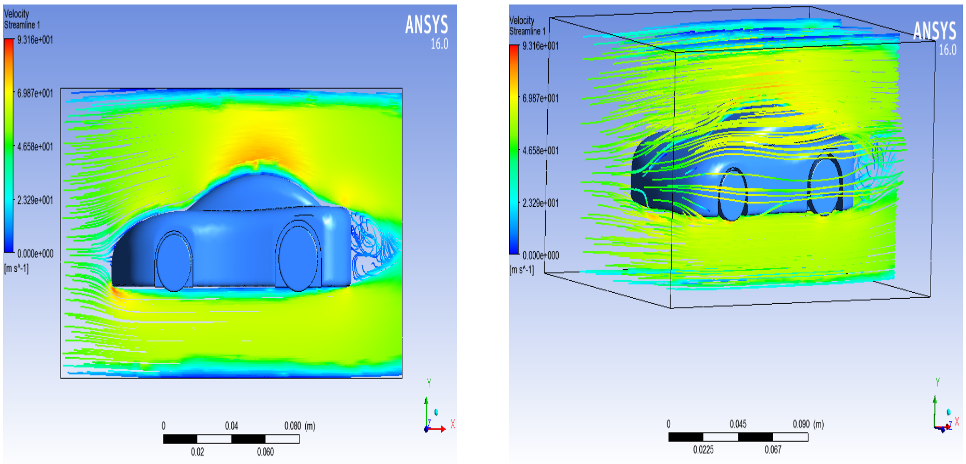

(a) (b)

Figure 11. Air velocity flow

4.2.2. Car Speed vs Voltage Generation

The following graph in Figure 13 was obtained as a result of comparison between the car speed and the voltages induced in the DC generator with and without load (car battery). It is observed that the voltage increases with the increase in the car's velocity. Without load, we obtain voltages as high as 35V at 90 km/hr, but in the presence of a load, this obtained voltage decreases to about 25V at the same velocity of 90km/hr. The regulated line in the given graph indicates the voltages obtained after they are passed through a DC regulator to stabilize them at a constant charging voltage, which is 14.6V for lead acid battery and this voltage is achieved at the speed of 45 km/hr.

4.2.3. Car speed vs Electrical parameters

On the basis of data gathered, it is observed that at 90km/hr, the generation system has a stable voltage of 14.6V with a charging rate of 6.9Ah. The curves indicates that with the increase in the velocity of the car the voltage and current are also increased gradually, except for voltage which stabilizes after required charging potential is achieved, as shown in Figure 14(a). At the speed rate of 90km/hr, the total power output obtained is approximately near to 100W as shown in Figure 14(b). It is to be mentioned that the charging rate can be increased with some adjustments, but it will jeopardize the life span of the battery.

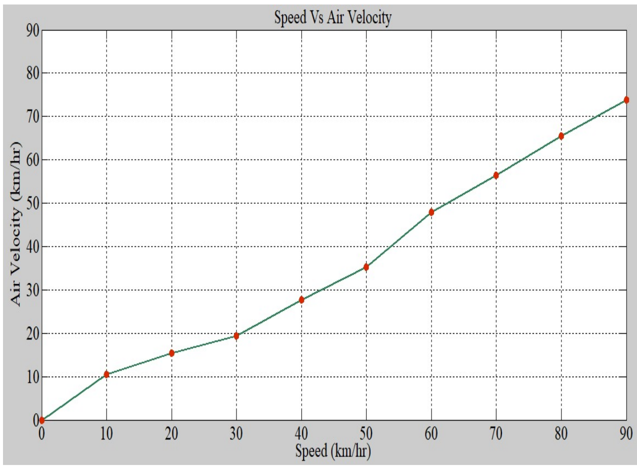

Figure 12. Car speed vs Air velocity

Preprints (www.preprints.org) | NOT PEER-REVIEWED | Posted: 9 July 2021 doi:10.20944/preprints202107.0214.v1

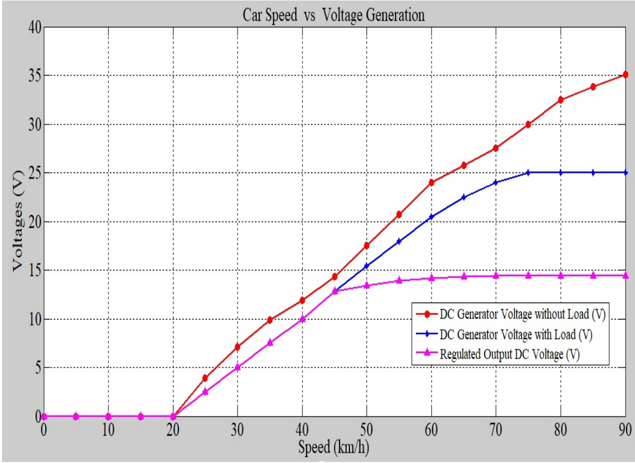

Figure 13. Car speed vs Voltage generation

4.2.4. Time vs Battery Charging Current

In the following graph in Figure 15, the timing of the battery charging is compared. This given graph basically shows the charging rate of battery from 9V (dead-battery) upto 13.1V (fully-charged) charging state of the battery. This is because of the battery resistance which varies. So, by this curve it is to be estimated that when the battery is in low charging condition it has high resistance and with the passage of time as the battery starts charging and ionizing its charges then the current increase with the decrease in the resistance. At one point maximum current drawn limit of the battery is achieved and then again resistance of the battery increases when it is going closer to the fully charged state.

5. System Efficiency Analysis

This analysis has been done so as to depict the conversion of energy from wind electrical form via different transformations. First of all, when the car is driven then the air strikes it. As the car has some velocity, the air coming towards it strikes it with some velocity too, but the air velocity is less than the speed of car thus the car keeps on moving in the forward direction. This shows that the work being done by the car is more as compared by the work done by the wind on the car.When the car gets driven, the wind strikes it with some velocity thus it exerts some force on the car. This air then gets diverted and moves on. Thus, it remains unused. In this research, a system is proposed which is using the energy of this wind which is striking the car. The wind with above-mentioned power will strike the wind turbine and transfer its power to it.

After some losses, this power then will become turbine power. This power of the turbine is so called because this is the energy with the wind turbine moves. Now, this rotating wind turbine has enough power to be used to do some work. Thus, this turbine is attached with a Permanent Magnet DC Motor, which has been used as a DC Generator in this article, with the help of a mechanical shaft. This rotating wind turbine power will be transferred to the DC Motor and its rotor will start moving. An important thing is that there are also some power losses during the transformation of energy from the wind turbine towards the motor.

So, now after all these transformations, the power that is now present is called Mechanical Power. This Mechanical Power tells us how much work is being done. As, in this case, it is a generator then it shows us the work being done by the Generator or specifically, by the rotor of the DC Generator. As in this case, the work is being done by the DC Generator, so it will convert the mechanical power into electrical power. Electrical Power is basically the measurement of the flow of current towards the load that is used for some purpose; in this case it is a 12V Lead Acid Battery. This electrical power, as given below, is directed towards the battery after some adjustments and protections. First of all, the DC voltages are regulated at a desired DC voltage so as to charge the battery at a constant voltage. Then

Preprints (www.preprints.org) | NOT PEER-REVIEWED | Posted: 9 July 2021 doi:10.20944/preprints202107.0214.v1

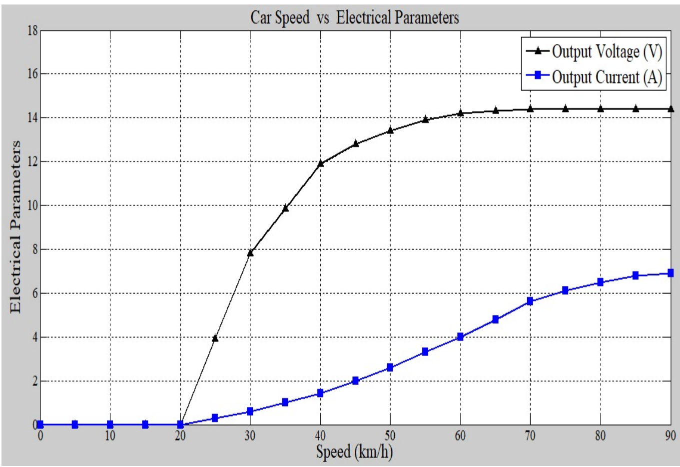

(a)

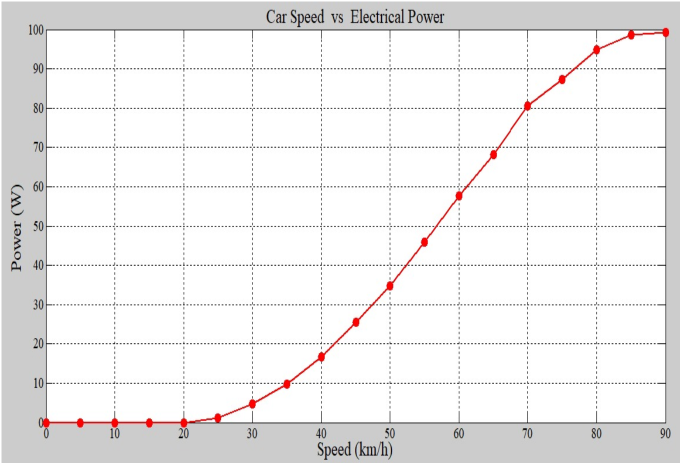

(b)

Figure 14. Car speed vs Electrical parameters

after using a protection circuitry, this electrical power is has been provided to the battery to be stored inside it so that when there is a need to use it, the battery can be a source for another load. The Figure 16 and Table 1 shows the system efficiency at different stages of power generation at air velocity of 18.2m/s and the losses occur at each stage and the final electrical output received after losses.

Table 1: Power evaluation at different stages.

Car Speed (km/hr)	Air Velocity (m/s)	Wind Power (W)	Turbine Power (W)	Mechanical Power (W)	Electrical Power (W)
10	2.90	1.4	0.4	0.4	0.4
20	4.30	4.6	1.4	1.3	1.3
30	5.40	9.1	2.7	2.7	2.6
40	7.70	26.4	8.0	7.8	7.5
50	9.80	54.6	16.6	16.1	15.6
60	13.3	133.5	41.5	40.3	39.1
70	15.7	224.4	68.3	66.4	64.4
80	18.2	343.8	106.4	103.4	100.3
90	20.5	499.3	152.4	147.7	143.4

Preprints (www.preprints.org) | NOT PEER-REVIEWED | Posted: 9 July 2021 doi:10.20944/preprints202107.0214.v1

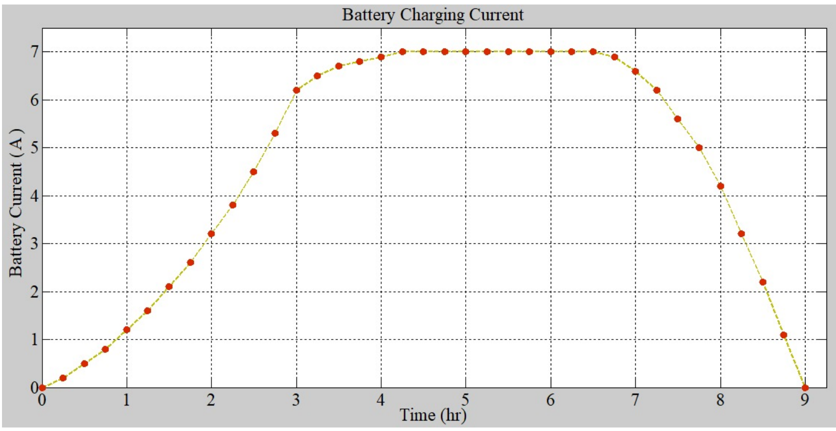

Figure 15. Time vs Battery Charging Current

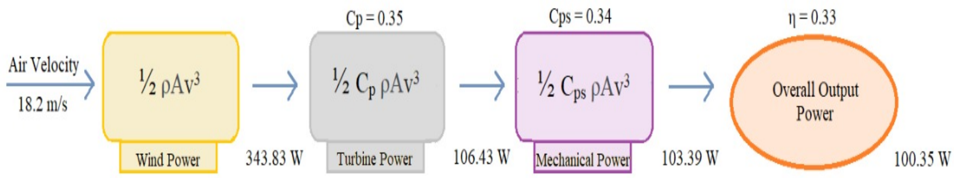

Figure 16. Efficiency of power generation at different stages

5.1. Betz Limit Analysis

As per Betz's law[38], no turbine can capture more than 16/27 (59.3%) of the kinetic energy in wind. The factor 16/27 (0.593) is known as Betz's coefficient. The Betz limit is based on an open-circle actuator. If a diffuser is utilized to gather extra wind stream and direct it through the turbine, more kinetic energy can be separated, yet the limit despite everything applies to the cross-sectional area of the whole structure.

According to the analysis done in this research, for the turbine of area(0.0791m), the betz limit efficiency is 30.3%. For a motor of the of 350W power, the overall system efficiency is 28.5%. This yield can be improved by increasing the area of the diffuser, but keeping in mind that the betz limit constraints are still in play.

5.2. Drag Coefficient Analysis

In the previous research work, which was based on the effect of drag coefficient on the car in the presence of a charging device on various location, it emphasizes the need for low or negligible drag force, that would add up in the original drag force due to the charging system installation. The conclusion from the research paper supported the theory that a charging system mounted on the front of the car bumper is a strong and promising location for maximum production and less drag at different positions of the car as shown in Table 2.

Table 2: Drag coefficient at car different position.

No.	Turbine Status	Drag Coefficient
1	Without wind turbine	0.39
2	At front of the car (bumper)	0.39
3	At hood of the car (bonnet)	0.45
4	At top of the car (roof)	0.51

5.3. Power Generation Analysis

According to the results gathered during analysis, the total power per hour was calculated to be approximately 100W, which is 28.5% efficient depending on the charging requirements of the battery. As per the motor configuration, the average power that can be produced by it is in between 15% to 35% of the total power. Keeping this information, it can be concluded that the power efficiency that has been acquired is among the favourable requirements.

5.4. Battery Discharge Time w.r.t Car Loads

As shown in given Table 3, more often used electrical loads of a car along with their power and current ratings have been discussed and on the basis of that, the rightmost column has been driven. This column basically shows the time required to discharge a fully charged 40 Ah battery, when each load is connected to it. These loads are of different types. First one is the lighting loads which include the headlights, back lights, and the hazard lights. Secondly, body electrical loads include the power window, wiper/washer system. The third type is media which includes video/audio systems, the navigation and GPS systems. Another type is the HVAC loads including the air compressor of the car.

The purpose of this analysis is to check the capability of the proposed system over-running loads of a car, on which it is installed. Keeping in view the electricity generation, a statistical approach has been used to estimate which loads of a car can be driven on a fully charged 40 Ah battery, charged using the proposed system. Moreover, if each of them is connected to the battery, how much time will be required to use battery completely? The Answer to this is in the rightmost column. Afterward, a very important analysis has been done. If all the loads excluding the air compressor are left to run on the battery with specifications mentioned above, then it would keep them running all these loads for about half an hour i.e. 0.52 hour (31 minutes). But, if the air compressor is included in the loads being driven over the battery, it can still keep all these loads running for about 0.34 hour i.e. 20 minutes.

Another very important discussion is that whether the proposed system is capable of running the below mentioned loads without a motor or not. Let us first see them separately. The blacklights and the hazard lights are those which can run directly on the proposed architecture while leaving some unused electrical behind. The headlights, power windows, and wiper washer system are the loads that will run with full generated power being utilized i.e. without leaving any extra electric power behind. As for the air compressor and the navigation and GPS systems are concerned, then they will not run merely on the direct supply of generated electric power. They will require some external electric supply as well. But, this generated electric power will be 20% and 40% of the power ratings of air compressor and navigation/GPS system. Thus, it will surely assist in reducing their dependence over any electric supply e.g. a battery. So, it can be concluded that the proposed system is generating enough electrical power to withstand the more often used loads of a car directly i.e. without using any battery.

5.5. Design and Cost Analysis

As a major objective of our research, the positioning of the fan was a vital aspect of analysis. The experimental results have shown a considerably better performance than the procedures used in previous papers. This proves our theory that the front position is the perfect spot for the adjustment of the wind turbine system for maximum utility. The fan used for wind generation worked satisfyingly with the given motor and circuit parameters. As a whole, the complete research including the hardware material for practical analysis was very cost-effective. All the material required for the testbed work was available in the local market and were cheap to buy, while also ensuring their precision and durability. As a team, it is our strong belief that in the future if an industrial version is created, the end product will be very user friendly in terms of the cost.

Preprints (www.preprints.org) | NOT PEER-REVIEWED | Posted: 9 July 2021 doi:10.20944/preprints202107.0214.v1

Table 3: Battery discharge time w.r.t loads.

Serial No.	Loads	Power (W)	Current (A)	Battery Discharged Time (hour)
1	Head-lights (2)	120	10	4.0
2	Back-lights (2)	50	4.1	9.1
3	Hazard-lights (4)	84	7.0	5.7
4	Power window (4)	120	10	4.0
5	Wiper and washer	140	9.8	4.0
6	Video and audio system	250	20.8	1.9
7	Navigation and GPS	150	12.5	3.2
	Subtotal	**914**	**76.1**	**0.52**
8	Air compressor	500	41.6	0.9
	Total	**1414**	**117.8**	**0.34**

6. Conclusion

With the surge to explore new dimensions to mitigate the carbon emissions, Today's smart cities are committed to increase their Low Emission Zones (LEZ) in an effort to replace the conventional gas vehicles with the electric vehicles, effectively meeting the requirements of several IoV use cases. To support the optimal operation, the design of wind power harvester is proposed and evaluated in this article. The aerodynamic drag and air speed qualities around the vehicle with a wind turbine framework were numerically researched. The vehicle model was simulated by Fluent module of ANSYS software to contemplate the wind stream trademark around the vehicle body and to decide the drag power of the vehicle at a specific speed. Furthermore, on the basis of the obtained results, practical evaluation analysis was also done in order to achieve the research objectives. After the simulated and practical experiments, the front bumper is recommended to be an ideal spot on the car for installing this kind of device for making an effective charging system of EVs. This article has rather focused on charging the EVs while utilizing their batteries considering a vechile speed range from 40 km/h to 90 km/h. This range can be improved by designing a DC Voltage Regulator capable of taking larger range of input voltages to be stabilized. The authors are committed to extend this work towards automating the energy generation process inducing integrated control and regulation of the generated voltage along with exploring different options to transfer surplus power to the national grid for general purpose utilization.

Conflicts of Interest: The authors declare no conflict of interest.

References

1. Raja, G.; Anbalagan, S.; Vijayaraghavan, G.; Dhanasekaran, P.; Al-Otaibi, Y.D.; Bashir, A.K. Energy-Efficient End-to-End Security for Software Defined Vehicular Networks. *IEEE Transactions on Industrial Informatics* **2020**.
2. Hussain, S.A.; Iqbal, M.; Saeed, A.; Raza, I.; Raza, H.; Ali, A.; Bashir, A.K.; Baig, A. An efficient channel access scheme for vehicular ad hoc networks. *Mobile Information Systems* **2017**, *2017*.
3. Sherazi, H.H.R.; Raza, I.; Chaudary, M.H.; Hussain, S.A.; Raza, M.H. Multi-radio over fiber architecture for road vehicle communication in VANETs. *Procedia Computer Science* **2014**, *32*, 1022–1029.
4. Iwendi, C.; Uddin, M.; Ansere, J.A.; Nkurunziza, P.; Anajemba, J.H.; Bashir, A.K. On detection of Sybil attack in large-scale VANETs using spider-monkey technique. *IEEE Access* **2018**, *6*, 47258–47267.
5. Azzaoui, N.; Korichi, A.; Brik, B.; el amine Fekair, M.; Kerrache, C.A. On the Communication Strategies in Heterogeneous Internet of Vehicles. The Proceedings of the Third International Conference on Smart City Applications. Springer, 2019, pp. 783–795.

6. Sherazi, H.H.R.; Khan, Z.A.; Iqbal, R.; Rizwan, S.; Imran, M.A.; Awan, K. A heterogeneous IoV architecture for data forwarding in vehicle to infrastructure communication. *Mobile Information Systems* **2019**, *2019*.
7. Kumar, A.; Hariharan, N. Enhanced Mobility Based Content Centric Routing In RPL for Low Power Lossy Networks in Internet of Vehicles. 2020 3rd International Conference on Intelligent Autonomous Systems (ICoIAS). IEEE, 2020, pp. 88–92.
8. Sherazi, H.H.R.; Imran, M.A.; Boggia, G.; Grieco, L.A. Energy harvesting in LoRaWAN: A cost analysis for the industry 4.0. *IEEE Communications Letters* **2018**, *22*, 2358–2361.
9. Sherazi, H.H.R.; Grieco, L.A.; Imran, M.A.; Boggia, G. Energy-Efficient LoRaWAN for Industry 4.0 Applications. *IEEE Transactions on Industrial Informatics* **2021**, *17*, 891–902. doi:10.1109/TII.2020.2984549.
10. Raja, G.; Dhanasekaran, P.; Anbalagan, S.; Ganapathisubramaniyan, A.; Bashir, A.K. SDN-enabled Traffic Alert System for IoV in Smart Cities. IEEE INFOCOM 2020-IEEE Conference on Computer Communications Workshops (INFOCOM WKSHPS). IEEE, 2020, pp. 1093–1098.
11. Sun, D.; Ou, Q.; Yao, X.; Gao, S.; Wang, Z.; Ma, W.; Li, W. Integrated human-machine intelligence for EV charging prediction in 5G smart grid. *EURASIP Journal on Wireless Communications and Networking* **2020**, *2020*, 1–15.
12. Karfopoulos, E.L.; Hatziargyriou, N.D. A multi-agent system for controlled charging of a large population of electric vehicles. *IEEE Transactions on Power Systems* **2012**, *28*, 1196–1204.
13. Xie, D.; Chu, H.; Lu, Y.; Gu, C.; Li, F.; Zhang, Y. The concept of EV's intelligent integrated station and its energy flow. *Energies* **2015**, *8*, 4188–4215.
14. Quartey, G.; Adzimah, S.K. Generation of electrical power by a wind turbine for charging moving electric cars. *J. Energy Technol. Policy* **2014**, *4*, 19.
15. Ohya, Y.; Karasudani, T. A shrouded wind turbine generating high output power with wind-lens technology. *Energies* **2010**, *3*, 634–649.
16. Sofian, M.; Nurhayati, R.; Rexca, A.; Syariful, S.S.; Aslam, A. An evaluation of drag coefficient of wind turbine system installed on moving car. Applied Mechanics and Materials. Trans Tech Publ, 2014, Vol. 660, pp. 689–693.
17. Bijlani, B.; Rathod, P.P.; Sorthiya, A.S. Experimental and Computational Drag Analysis of Sedan and Square-Back Car. *International Journal of Advanced Engineering Technology* **2013**, *4*, 63–65.
18. Awal, M.R.; Jusoh, M.; Sakib, M.N.; Hossain, F.S.; Beson, M.R.C.; Aljunid, S.A. Design and implementation of vehicle mounted wind turbine. *ARPN J Eng Appl Sci* **2015**, *10*, 8699–8860.
19. Zakaria, M.Y.; Pereira, D.A.; Hajj, M.R. Experimental investigation and performance modeling of centimeter-scale micro-wind turbine energy harvesters. *Journal of wind engineering and industrial aerodynamics* **2015**, *147*, 58–65.
20. Karthikeyan, N.; Murugavel, K.K.; Kumar, S.A.; Rajakumar, S. Review of aerodynamic developments on small horizontal axis wind turbine blade. *Renewable and Sustainable Energy Reviews* **2015**, *42*, 801–822.
21. Kishore, R.A.; Priya, S. Design and experimental verification of a high efficiency small wind energy portable turbine (SWEPT). *Journal of wind engineering and industrial aerodynamics* **2013**, *118*, 12–19.
22. Lu, L.; Han, X.; Li, J.; Hua, J.; Ouyang, M. A review on the key issues for lithium-ion battery management in electric vehicles. *Journal of power sources* **2013**, *226*, 272–288.
23. Sankardoss, V.; Geethanjali, P. PMDC motor parameter estimation using bio-inspired optimization algorithms. *IEEE Access* **2017**, *5*, 11244–11254.
24. Guldemir, H. Modeling and sliding mode control of dc-dc buck-boost converter. Proc. 6th Int. advanced technological Symp, 2011, Vol. 4, pp. 475–480.
25. Hannan, M.A.; Lipu, M.H.; Hussain, A.; Mohamed, A. A review of lithium-ion battery state of charge estimation and management system in electric vehicle applications: Challenges and recommendations. *Renewable and Sustainable Energy Reviews* **2017**, *78*, 834–854.
26. Ceraolo, M. New dynamical models of lead-acid batteries. *IEEE transactions on Power Systems* **2000**, *15*, 1184–1190.
27. Bezanilla, F. The voltage sensor in voltage-dependent ion channels. *Physiological reviews* **2000**, *80*, 555–592.
28. Singh, S.; Bhullar, S. Hardware implementation of auto switching and light intensity control of LED lamps. *Balkan Journal of Electrical and Computer Engineering* **2016**, *4*, 67–71.
29. Vobecky, J.; Hazdra, P.; Homola, J. Optimization of power diode characteristics by means of ion irradiation. *IEEE Transactions on Electron Devices* **1996**, *43*, 2283–2289.
30. Gunn, C.N.; Harding, S.J.; Ricci, M.A.; Loewen, D.N.; Cowan, P.C.; Hancock, M.A. Current sensor assembly, 2009. US Patent 7,557,563.
31. Babir, M.R.N.; Al Mahmud, S.A.; Mostary, T. Efficient M-QAM Digital Radio over Fiber System for Vehicular ad-hoc Network. 2019 International Conference on Robotics, Electrical and Signal Processing Techniques (ICREST). IEEE, 2019, pp. 34–38.
32. Munshi, A.; Unnikrishnan, S. Vehicle to Vehicle Communication Using DS-CDMA Radar. *Procedia Computer Science* **2015**, *49*, 235–243.
33. Manyonge, A.W.; Ochieng, R.; Onyango, F.; Shichikha, J. Mathematical modelling of wind turbine in a wind energy conversion system: Power coefficient analysis. *Applied mathematical sciences* **2012**, *6*, 4527–4536.
34. Ochieng, R.; Ochieng, R. ANALYSIS OF THE BETZ CRITERION IN WIND TURBINE POWER MODELLING BY USE OF "VARIATIONAL PRINCIPLE (METHOD)" IN THE POWER EQUATION. *International Journal of Energy, Environment and Economics* **2015**, *23*, 283.

35. Castelli, M.R.; De Betta, S.; Benini, E. Effect of blade number on a straight-bladed vertical-axis Darreius wind turbine. *World Academy of Science, Engineering and Technology* **2012**, *61*, 305–3011.
36. Hegde, S.S.; Thamban, A.; Bhai, S.P.M.; Ahmed, A.; Upadhyay, M.; Joishy, A.; Mahalingam, A. Highway mounted horizontal axial flow turbines for wind energy harvesting from cruising vehicles. ASME International Mechanical Engineering Congress and Exposition. American Society of Mechanical Engineers, 2016, Vol. 50596, p. V06BT08A043.
37. Fotso, B.M.; Nguefack, C.F.; Talawo, R.C.; Fogue, M. Aerodynamic analysis of an electric vehicle equipped with horizontal axis savonius wind turbines. *International Journal of Recent Trends in Engineering & Research (IJRTER)* **2019**, *5*, 17–26.
38. Gorban', A.N.; Gorlov, A.M.; Silantyev, V.M. Limits of the turbine efficiency for free fluid flow. *J. Energy Resour. Technol.* **2001**, *123*, 311–317.